Environment. Technology. Resources. Rezekne, Latvia
Proceedings of the 14th International Scientific and Practical Conference. Volume 3, 344-350

Investigating the Contrast of Surface Marking on Different Color Connectors for Telecommunications Needs

Daniels Raubiška
Faculty of Engineering
Rezekne Academy of Technologies
Rezekne, Latvija
e-mail: dr17057@edu.rta.lv

Imants Adijāns
Faculty of Engineering
Rezekne Academy of Technologies
Rezekne, Latvija
imants.adijans@rta.lv

Emil Yankov
Faculty of Engineering
Rezekne Academy of Technologies
Rezekne, Latvija
emil.yankov@rta.lv

Lyubomir Lazov
Faculty of Engineering
Rezekne Academy of Technologies
Rezekne, Latvija
lyubomir.lazov@rta.lv

Abstract. **The development of marking technologies for telecommunications connectors requires increasingly detailed information about their applications. One solution is to use QR codes that contain sufficient information about the connectors' applications. Accurate marking of connectors requires a precise marking system, such as a laser marking system. In this study, a Rofin PowerLine F20 Varia fiber laser was used to mark four different types of ABS plastic connectors in various colors. To achieve optimal marking for all four colors, three experiments were conducted to achieve contrasting marking and high roughness. Easy QR code reading was achieved with an average marking power of 3 W to 4.2 W, a laser marking speed of 300 mm/s to 500 mm/s, and a scanning frequency of 50 kHz to 70 kHz at a constant pulse duration of 8 ns and raster spacing of 50 µm. The microstructural changes and change in roughness were determined using a laser scanning microscope (Olympus OLS5000), which revealed structural changes on the surface and an increase in relative roughness from 39% to 76%. This experiment shows that different parameters of the laser marking mode are required for each color.**

Keywords: ABS plastic, Contrast, Fiber laser marking, QR code, Roughness.

I. INTRODUCTION

Labeling is used for various goods and products today. It is necessary to identify parts and different products. Thanks to the marking, the manufacturer controls the quality of the product and the consumer has the opportunity to obtain a quality guarantee, as well as to find out the characteristics and parameters of the purchased goods. Laser marking of materials is most often used in companies, because it is the fastest and most efficient way to mark products in large volumes [1]-[2]. Also, laser marking leaves a deep mark on the product, which is standard in many industries. Therefore, these marks cannot be removed without mechanical damage to the product. That is why the company can prevent unauthorized access to the product, mark the expiration date and improve the quality of the product. For example, a quick response (QR) code, which is a two-dimensional matrix barcode containing information about the object to which it is attached, can be used for this purpose. A QR code uses four standardized encoding modes (numeric, alphanumeric, binary, and kanji) to efficiently store data [3]. Laser marking is based on changes in the surface structure of the material being processed. Usually, this process is associated with the evaporation of material particles, as a result of which the marking appears as an indentation on the surface of the material. There is also another marking method, when the surface of the material is melted, in this way the morphological and structural changes of the surface occur, which creates a strongly pronounced marking effect [4].

Print ISSN 1691-5402
Online ISSN 2256-070X
https://doi.org/10.17770/etr2023vol3.7263

Laser marks can be obtained using both thermal and thermal modes of beam-material interaction. Each thermal mechanism is characterized by a temperature rise that ranges from heating, melting, and vaporization [5]-[6]. The effects of material properties (such as absorptivity and melting point) and marking parameters (such as power density, focal position and marking speed) on mark readability characteristics (such as mark contrast and mark width) are reviewed [7]-[8]. Advances in direct laser marking of plastics provide unprecedented marking quality, contrast and speed. When used correctly, laser marking can provide many manufacturing benefits and improve product appearance and function [9]. To obtain high-quality images, knowledge of the interaction of the laser with plastic is necessary. [10]-[11]. A fiber laser was used for the experiments, it is a class of solid-state lasers in which the amplification medium is an optical fiber. Fiber lasers have been a key technology in the field of solid-state lasers since the first proposal to use an optical fiber as a laser mode selector. Stimulated emissions from the amplifying fiber coherently amplify the signal as the signal oscillates between two signal reflectors [12]-[13].

The purpose of the present study is to determine the influence of the color of the surface of the studied samples (telecommunications connectors), how it affects the marking process under the same conditions, technological parameters of the laser.

II. Materials and Methods

ABS (acrinotrile-butadiene styrene) plastic-impact-resistant technical thermoplastic resin based on acrylonitrile copolymer with butadiene and styrene was used for the experiments. The proportions vary: 15 - 35 % acrylonitrile, 5 - 30 % butadiene and 40 - 60 % styrene. A characteristic softening temperature is 150 - 160 °C and a boiling point of 245 °C. This material is actively used in many industrial and scientific sectors.

Fig. 1. Determining the value of the contrast marking on collor connectors using Photoshop.

This material is actively used in many industrial and scientific sectors, such as chemical industry, construction industry, automobile industry, household appliances, electronic connecting connectors and other related fields [14]-[16]. Plastic connectors designed for optical fibers with four different colors - blue, cream, green and fuchsia - were used for the research (Fig.1).

The goal is to establish laser marking modes that provide contrast with an easily readable Q code. The Rofin PowerLine F20 Varia laser system (Fig.2) with a wavelength of 1064 nm was used for the experiments. The technological capabilities of the system are average power 20 W, pulse duration from 4 to 200 ns and pulse repetition frequency from 2 to 1000 kHz, line step from 1 µm to 120 mm and speed from 1 mm/s to 2000 mm/s. The maximum marking area is 120 mm × 120 mm.

Fig. 2. Fiber laser Rofin PowerLine F20 [17].

Three marking constant parameters are pulse duration 8 ns and line pitch 5 µm, diameter of working spot d = 40 µm, defocusing Δf = 0 mm and number of repetitions 1 for the fabricated matrices. In the first experiment, three marking speeds 300 mm/s, 400 mm/s, and 500 mm/s were selected, where the pulse energy (Ep) (1) and peak power (P_p) (2) were constant 60 µJ and 7.5 kW, respectively and line density N_x 20 µm^{-1} (3), intensity (I_p) 11.94 W/µm² (5), energy or fluence (F_p) 0.096 µJ/µm² (6). The pulse density (N_y) (4) values for the three speeds are changed to 200 mm^{-1}, 150 mm^{-1} and 120 mm^{-1}, respectively.

$$E_p = \frac{P}{f}\,[\mu\mathrm{J}] \tag{1}$$

$$P_p = \frac{E_p}{\tau}\,[\mathrm{kW}] \tag{2}$$

$$N_x = \frac{1}{\Delta x}\,[\mathrm{mm}^{-1}] \tag{3}$$

$$N_y = \frac{f}{v}\,[\mathrm{mm}^{-1}] \tag{4}$$

$$I_p = \frac{2\times P_p}{\pi\times w^2}\,[\mathrm{W}/\mu\mathrm{m}^2] \tag{5}$$

$$F_p = \frac{2\times E_p}{\pi\times w^2}\,[\mu\mathrm{J}/\mu\mathrm{m}^2] \tag{6}$$

$$E_{ef} = \frac{P\times f}{v^2}\,[\mu\mathrm{J}] \tag{7}$$

Where E_p – pulse energy, P - average power, f - scanning frequency, P_p - peak power, τ - pulse duration, Δx - line pitch, v - scanning in marking speeds, Ip – intensity, w - focal spot radius, F_p - density or fluence and E_{ef} - efficient energy.

In the second experiment, the changing parameter is the scanning frequency 50 kHz, 60 kHz and 70 kHz and the scanning speed is a constant 400 mm/s. In this case, the pulse energy (E_p) 60 µJ and peak power (P_p) change and 7.5 kW, respectively. The parameter line density (N_x) 20 mm^{-1}, intensity (I_p) according to the scanning frequency respectively 11.94 W/µm², density or fluence (Fp) 0.096 µJ/µm². The values of pulse density (N_y) for the three frequencies change to 125 mm^{-1}, 150 mm^{-1} and 175 mm^{-1}, respectively.

In the third experiment, the average power (P) is changed by 50 %, 60 % and 70 % (3.0 W, 3.6 W and 4.2 W). In an experiment, it will lead to constant values of pulse density (N_y) 150 mm^{-1} and line density (N_x) 20 mm^{-1} for the three average powers. For pulse energy (E_p), peak power (P_p), intensity (I_p) and density or fluence (F_p) change depending on the average power (P) 3.0 W, 3.6 W and 4.2 W respectively pulse energy (E_p) 50 µJ, 60 µJ and 70 µJ, peak power (P_p) 6.25 kW, 7.5 kW and 8.75 kW, intensity I_p 9.95 W/µm², 11.94 W/µm² and 13.93 W/µm², density or fluence F_p 0.0796 µJ/µm², 0.0955 µJ/µm² and 0.1115 µJ/µm².

After laser marking, the colored connectors (Fig.1) were scanned with a 2D scanner HP Scanjet G3010 to determine the contrast. To get my good image, the scan mode was at 2400 dpi, contrast 80 % and saved in *.tiff format. The digital image is inserted into Photoshop to measure the resulting mark. Sampling of the unmarked and marked area is done at an area of 11x11 pixels in order to average the measurement. The obtained values for each measured area are recalculated according to equation (8) for contrast against the background in percentages:

$$k* = \frac{N_n - N_f}{N_f} \times 100\% \qquad (8)$$

where N_f is measured background value, N_n measured value in a laser-marked area.

Roughness measurements and the resulting microstructure were examined with an Olympus model "OLS5000" laser microscope (Fig.3). The obtained microstructural images were carried out using a 10× objective, magnification 227×, as the examined area for each measurement 1280×1280 µm with a measurement accuracy of ± 2.0 µm. From the obtained 3D images with the laser system of the microscope, the roughness R_a and R_z perpendicular to the marking lines with a length of 1280 µm, and the roughness R_q for the entire examined area 1280×1280 µm were measured. The obtained values are plotted in tables and graphical dependences of changes in roughness depending on speed and step during surface laser processing are shown. The built dependencies are presented in the results.

Fig. 3. Olympus OLS5000 [18].

Determination of the percentage change in roughness after laser marking is determined by the dependence:

$$R^* = \frac{R_n - R_f}{R_f} \times 100\% \qquad (9)$$

where: R_n is the roughness in the laser marked area, R_f is the roughness in the unmarked area of the sample.

III. Results and discussion

For the contrast analysis, comparison plots were constructed for the three experiments of the four colors connectors and presented in (Fig.4) for the effect of the average power on laser marking, (Fig.5) for the effect of speed on laser marking and (Fig.6) for the effect of the frequency of laser marking.

A. The influence of power on contrast

With changing average power, it is found that the connector with Cream color has the highest contrast reaching from 39.58 % to 46.88 % compared to the background (Fig.4). A high contrast value is achieved at a power of 4.2 W. With the blue connector, maximum contrast (16.67 %) against the background is also achieved at the maximum experimental power (4.2 W). With the remaining two connectors Green and Fuchsia, the maximum contrast is obtained at 3.6 W, 27.94 % and 21.95 %, respectively. It should be noted that the resistor needs to be tested at higher wattages than 4.2 W for the Blue and Cream connectors.

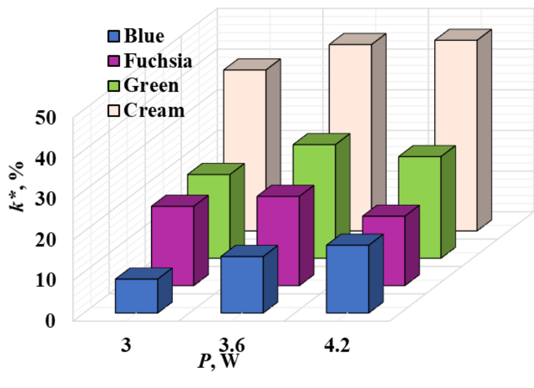

Fig.4. Comparison of power contrast.

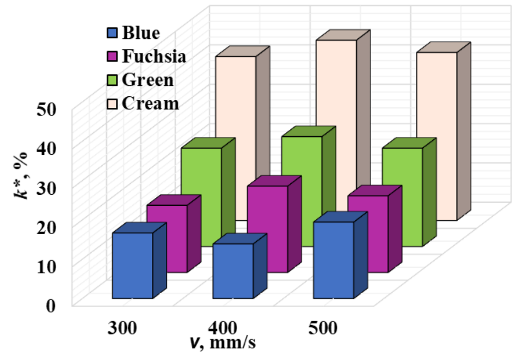

Fig.5. Comparison of speed contrast.

B. The influence of speed on contrast

In the varying laser marking speed experiment, high contrast for the Cream, Green and Fuchsia connectors is obtained at a speed of 400 mm/s (Fig.5). While for the blue connector, maximum contrast is obtained at a speed of 500 mm/s. The highest contrast is again obtained for the connector with the color Cream 45.83 %, then for Green 27.94 % and Fuchsia 21.95 %. The pro blue connector has a contrast of 19.44%, which is the lowest value compared to the other connectors. And in this experiment, it is necessary to investigate at higher speeds to obtain a higher contrast of the blue connector.

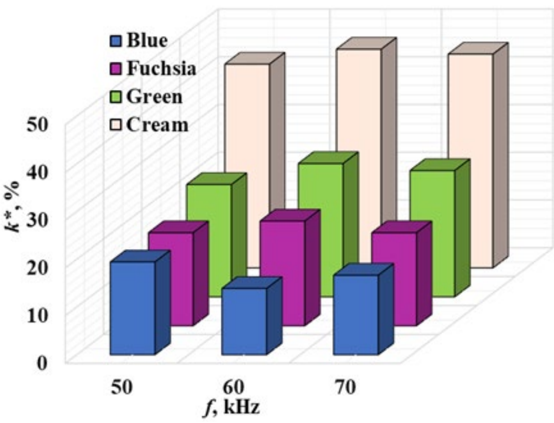

Fig.6. Comparison of frequency contrast.

C. The influence of frequency on contrast

In the last experiment for climbing marking of colored connectors with varying scanning frequencies of 50 kHz, 60 kHz and 70 kHz, comparative contrast variation diagrams were constructed and presented in (Fig.6). At 60 kHz, the Cream, Green and Fuchsia connectors have maximum contrast, and the blue connector at 50 kHz. In the third experiment, the Cream color connector has the highest contrast 45.83 %. Next with high contrast is the connector with the color Green 27.94 %, and Fuchsia has a contrast of 21.95 %. The lowest contrast is again obtained for the blue connector 19.40 %, but this is the highest value at the three frequencies examined. In order to increase the resistance of the blue connector, it is necessary to conduct experiments at lower frequencies, which tendency is also established by the graphical dependence (Fig. 6).

The change in the roughness after laser marking compared to the roughness before marking also has an effect on the easy reading of the marking. For this purpose, comparative diagrams were built for the four colored connectors when the average power varied from 3.0 to 4.2 W (Fig.7), the speed from 400 to 600 mm/s (Fig.8) and the frequency from 50 to 70 kHz (Fig.9).

D. The influence of power on roughness

The results of the comparison with power variation show that the power variation affects the roughness of the connectors (Fig.7). The highest percentage of change in roughness is found for the Cream connector $R_z* = 99.44$ % at an average power of 4.2 W. In this case, the effective energy is the highest (E_{ef} = 1.58 μJ) for the conducted experiment. For the connector with blue color, the highest roughness is also achieved at 4.2 W ($R_z* = 55.50$ %), and the effective energy is the same (Tabl.1). An interesting trend for the variation of roughness is obtained for the Fuchsia color connector, with the maximum roughness being achieved at a lower average power of 3 W, where $R_z* = 45.12$ %. As the power increases to 4.2 W, the roughness decreases to $R_z* = 8.93$ %. The maximum effective energy for high roughness in this experiment is 1.13 μJ at a core power of 3 W.

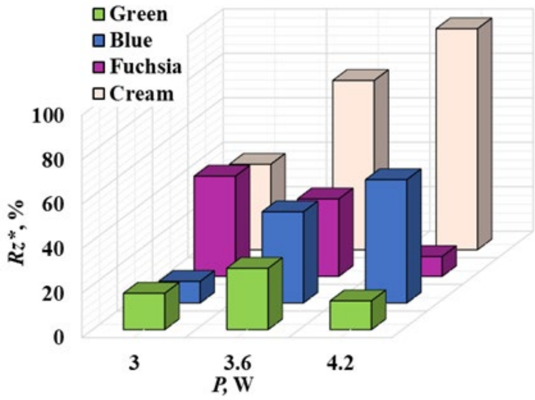

Fig.7. Surface roughness at average power changes.

With the Green connector, the maximum roughness ($R_z* = 27.59$ %) is achieved at an average power of 3.6 W, where the effective energy is 1.35 μJ. At the remaining two power values, the roughness is lower. For reading the mark in this power change experiment, one can mainly rely on the resulting contrast mark and good roughness. The main reason for the increase in roughness is the increase in pulse energy (E_p), peak power (P_p) and intensity (I_p) and density or fluence (F_p) with an increase in average power.

TABLE 1. CHANGE OF EFFECTIVE ENERGY ACCORDING TO THE AVERAGE POWER, SCAN FREQUENCY AND SPEED SCANNED

	P **(W)**			***f*** **(kHz)**			**v (mm/s)**		
	3	**3.6**	**4.2**	**50**	**60**	**70**	**300**	**400**	**500**
E_{ef}, μJ	1.13	1.35	1.575	0.9375	1.125	1.3125	2.4	1.35	0.864

E. The influence of speed on roughness

In the experiment with varying the speed of 300 mm/s, 400 mm and 500 mm/s, the roughness is varied according to the color of the connector (Fig.8). At the low scan speed of 300 mm/s, the Blue and Green connectors have the highest roughness changes, R_z* = 47.75 % and R_z* = 39.71 %, respectively, where the effective energy in this experiment is 2.4 µJ. With the Cream connector, the maximum roughness (R_z* = 76.16 %) is obtained at a scanning speed of 400 mm/s, which is the highest for the entire experiment. The effective energy at this rate is 1.35 µJ. For the Fuchsia connector, the roughness variation has the lowest values for the experiment. A maximum value of the roughness (R_z* = 35.05 %) is obtained at 500 mm/s, where the effective energy is lowest for the experiment 0.864 µJ. This shows that for the Fuchsia connector, the absorbed energy at constant values of 60 kHz and average power of 3.6 W results in lower roughness changes.

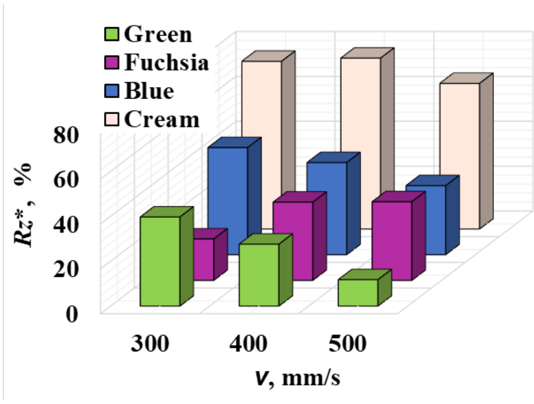

Fig.8. Surface roughness for speed change.

F. The influence of frequency on roughness

In a frequency change experiment, a variable parameter is the pulse density in line (N_y), which at 50 kHz is 125 mm^{-1}, 60 kHz is 150 mm^{-1}, and 70 kHz is 175 mm^{-1}. This change in pulse density in a line affects the change in roughness. The highest relative roughness change from baseline roughness in this experiment is achieved at the 70 kHz scan rate for the Blue, Cream, and Fuchsia connectors, where R_z* = 49.48 %, R_z* = 76.73 %, and R_z* = 67.41 % respectively (Fig.9). In this frequency scan, the ejective energy is the highest for the experiment 1.3125 µJ. Unlike the other connectors, the Green connector has maximum roughness at 60 kHz (R_z* = 27.59 %), where the effective energy is lower at 1.125 µJ. And in this experiment, the lowest values for change in roughness are found at the Green connector. All color connectors in this experiment have a result exceeding 10 % of the usable roughness. This result shows that the reading of the laser marking can be relied on the obtained contrast between the background and the marking and the resulting increased roughness.

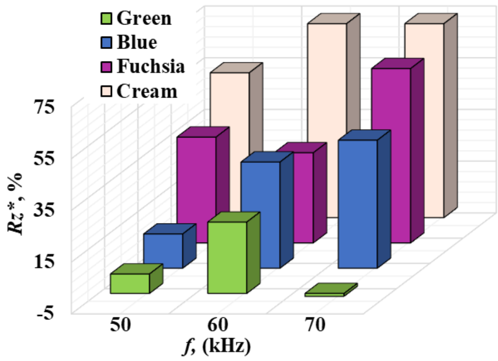

Fig. 9. Surface roughness at frequency changes.

From the laser marking experiments performed, modes were selected that gave high contrast and large roughness variation for each connector. Developed a QR code for laser marking, exploiting the established optimal modes for easy reading. In (Fig.10) the marked connectors with a developed QR code are presented.

Fig. 10. Marking the QR code.

From the marking readability check, it was found that reading the markings for the Blue, Cream and Fuchsia connectors was very easy. While the Green color connector is difficult to read. In order to determine the reason for the difficult reading, all connectors were measured for roughness changes with an Olympus OLS5000 scanning microscope, and the results are presented in (Fig.11-14). From the measurement, it is found that the roughness (R_z) of the Blue, Cream and Fuchsia connectors are R_z = 2.089 µm, R_z = 8.875 µm and R_z = 3.009 µm respectively. While the Green connector has the lowest R_z = 1.957 µm.

To improve readability, an experiment was conducted with two repetitions of marking, and the measured roughness increased to Green R_z = 12.108 µm (Fig.15), and the contrast also improved. The (Fig.15) shows traces of melting with modification of the surface roughness. This made it possible to easily read the marking of QR code.

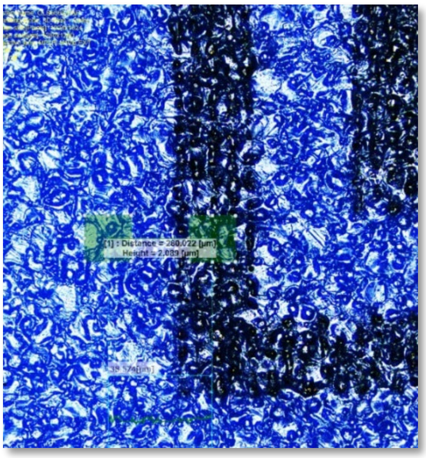

Fig. 11. Roughness connector Blue.

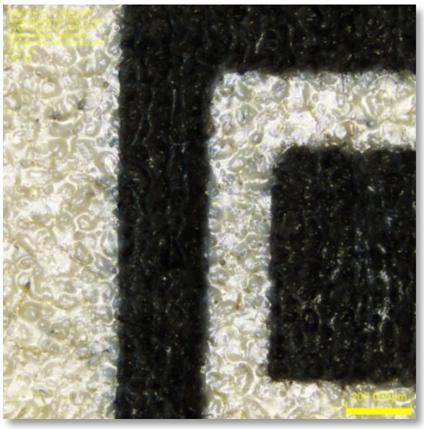

Fig.12. Roughness connector Cream.

Fig.13. Roughness connector Green.

Fig.14. Roughness connector Fuchsia.

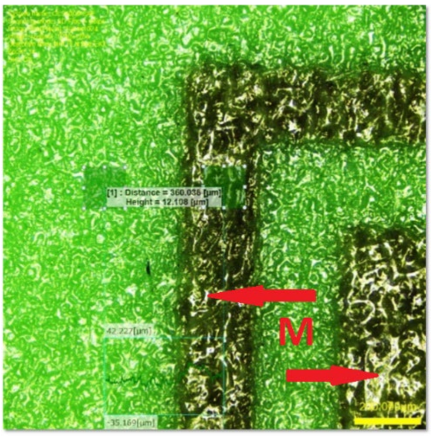

Fig.15. Roughness connector Green, M-melting.

IV. CONCLUSIONS

The following conclusions and findings can be made from the conducted scientific research:

- Different laser marking input parameters are required to obtain a contrast marking of QR code on a Blue, Cream, Fuchsia and Green color connector.
  - The highest contrast (k^* = 83.75 %) is found at Cream connector at P = 4.2 W, v = 400 mm/s and f = 60 kHz, where Ep = 70 µJ, P_p = 8.75 kW, I_p = 0.0139 W/µm^2, F_p = 0.1115 µJ/µm^2, E_{ef} = 1.575 µJ;
  - With a Green connector, the measured contrast (k^* = 27.94 %), which is achieved at laser surface marking parameters P = 3.6 W, v = 400 mm/s and f = 60 kHz, where Ep = 60 µJ, P_p = 7.5 kW, I_p = 0.0119 W/µm^2, F_p = 0.0955 µJ/µm^2, E_{ef} = 1.35 µJ. This laser marking result was not satisfactory for the easy reading of the QR mark. During laser marking with two passes, the contrast reached values of k^* = 48.10 %, which created a prerequisite for easier reading of the QR code.
  - With connector Fuchsia contrast reaches maximum value (k^* = 52.70 %) at laser marking parameters P = 3.6 W, v = 400 mm/s and f = 60 kHz, where Ep = 60 µJ, P_p = 7.5 kW, I_p = 0.0119 W/µm^2, F_p = 0.0955 µJ/µm^2, E_{ef} = 1.35 µJ;

- The maximum contrast at the blue connector (k^* = 59.30 %) is found at laser marking parameters, P = 3.5 W, v = 500 mm/s and f = 50 kHz, where Ep = 70 µJ, P_p = 8.75 kW, I_p = 0.0139 W /µm^2, F_p = 0.1115 µJ/µm^2, E_{ef} = 0.70 µJ.

- In order to improve the readability of the QR code marking, the relative roughness (Rz*) has also been found to have an effect. To achieve a relative roughness (R_z*) change of more than 10 %, different laser marking input parameters are required for the four color connectors.
  - The largest relative roughness change (R_z* = 76.73 %) is for the Cream connector at P = 4.9 W, v = 400 mm/s, and f = 70 kHz, where E_p = 70 µJ, P_p = 8.75 kW, N_y = 175.0 mm^{-1}, I_p = 0.0139 W/µm^2, F_p = 0.1115 µJ/µm^2, E_{ef} = 2.1438 µJ.
  - A large relative roughness change (R_z* = 49.48 %) for the Blue connector is achieved in laser marking mode P = 4.9 W, v = 300 mm/s, and f = 70 kHz, where E_p = 70 µJ, P_p = 8.75 kW, N_y = 233.33 mm^{-1}, I_p = 0.0139 W/µm^2, F_p = 0.1115 µJ/µm^2, E_{ef} = 3.8111 µJ;
  - High relative roughness change (R_z* = 67.41 %) for Fuchsia connector is achieved in laser marking mode P = 4.2 W, v = 500 mm/s, and f = 70 kHz, where E_p = 60 µJ, P_p = 7.5 kW, N_y = 140.0 mm^{-1}, I_p = 0.0119 W/µm^2, F_p = 0.0955 µJ/µm^2, E_{ef} = 1.176 µJ;
  - Possible high relative roughness change (R_z* = 39.71 %) for Green connector is achieved in laser marking mode P = 3.6 W, v = 300 mm/s, and f = 60 kHz, where E_p = 60 µJ, P_p = 7.5 kW, N_y = 200.0 mm^{-1}, I_p = 0.0119 W/µm^2, F_p = 0.0955 µJ/µm^2, E_{ef} = 2.40 µJ.

These target castings give a clear idea that the color of the connector affects the modified contrast and roughness, which is directly related to the amount of absorption (absorption) and reflection of the effective energy. Further studies are needed to determine the optimal laser marking modes for high contrast and rudeness. It is necessary to determine how the overlap parameters in pulse overlap (K_{ov}) and coefficient of overlap between lnie (K_{soc}) affect the contrast of the marking and roughness. It is unassailable to establish the softening limits for the four connector colors when examining average powers, scan rates, and marking speeds.

ACKNOWLEDGMENT

The authors gratefully acknowledge financial support by the European Regional Development Fund, Postdoctoral research aid Nr. 1.1.1.2/16/I/001 research application "Analysis of the parameters of the process of laser marking of new industrial materials for high-tech applications, Nr. 1.1.1.2/VIAA/3/19/474".

REFERENCES

[1] F. Bravo-Montero, D. Castells-Rufas and J. Carrabina, High-speed laser marking with diode arrays, Optics & Laser Technology, Volume 146, 2022, https://doi.org/10.1016/j.optlastec.2021.107551.

[2] C. Lin, X. Shen, B. Hua and Z. Wang, Three-dimensional polarization marked multiple-QR code encryption by optimizing a single vectorial beam, Optics Communications, Volume 352, pp. 25-32, 2015, https://doi.org/10.1016/j.optcom.2015.04.068.

[3] R. Kikuchi, S. Yoshikawa, P. K. Jayaraman, J. Zheng and T. Maekawa, Embedding QR codes onto B-spline surfaces for 3D printing, Computer-Aided Design, Volume 102, pp. 215-223, 2018, https://doi.org/10.1016/j.cad.2018.04.025.

[4] В. И. Семашко, МЕТОДЫ ЛАЗЕРНОЙ МАРКИРОВКИ, Докады - БГУИР, Минск, Беларусь 2004. [Online]. Available: https://cyberleninka.ru/article/n/metody-lazernoy-markirovki/viewer [Accessed May 1, 2023].

[5] J. C. Ion, Chapter 15, Laser Processing of Engineering Materials, Butterworth-Heinemann, 2005, pp. 384-394.

[6] E. Hadizadeh, S. Pazokifard, S.M. Mirabedini and H. Ashrafian, Optimizing practical properties of MMA-based cold plastic road marking paints using mixture experimental design, Progress in Organic Coatings, Volume 147, 2020, https://doi.org/10.1016/j.porgcoat.2020.105784.

[7] Y. M. Noor, S. C. Tam, L. E. N. Lim and S. Jana, A review of the Nd: YAG laser marking of plastic and ceramic IC packages, Journal of Materials Processing Technology, Volume 42, Issue 1, Pages 95-133, 1994, https://doi.org/10.1016/0924-0136(94)90078-7.

[8] P. Narica and J. Fedotovs, Laser Marking of a Small Sized QR Code on a Plastic Surface, Reliability and Statistics in Transportation and Communication, vol 117, pp 418–429, Springer, March 2020, https://doi.org/10.1007/978-3-030-44610-9_41.

[9] M. A. Salim, Z. H. Termiti and A. Md. Saad, Mechanical Properties on ABS/PLA Materials for Geospatial Imaging Printed Product using 3D Printer Technology, Reference Module in Materials Science and Materials Engineering, Elsevier, 2019, https://doi.org/10.1016/B978-0-12-803581-8.11357-8.

[10] S. R. Sabreen, "Basic Material Science for Plastics Laser Marking" The Sabreen Group, Inc. January 2009, https://plasticsdecorating.com/articles/2009/basic-material-science-for-plastics-laser-marking/ [Accessed May 1, 2023].

[11] R. L. Stevenson, Implementation of Beam-Steered Laser Marking of Coated and Uncoated Plastics, Coloring Technology for Plastics, pp. 309-315, 1999, https://doi.org/10.1016/B978-188420778-5.50040-1.

[12] "Fiber laser", FiberLabs Inc., July 2021, https://www.fiberlabs.com/glossary/fiber-laser/ [Accessed May 1, 2023].

[13] N. Angelov, Investigation the Influence of the Number of Repetition and Volumetric Energy Density on Laser Marking of Products, Contemporary Materials, V−2, pp. 251-253, 2014, DOI:10.7251/COMEN1402250A

[14] S. Olivera, H. B. Muralidhara, K.Venkatesh, et al., Plating on acrylonitrile–butadiene–styrene (ABS) plastic: a review. J Mater, vol 51, pp. 3657–3674, January 2016, https://doi.org/10.1007/s10853-015-9668-7.

[15] C. Lavieja, M. J. Clemente, L. Oriol and J. I. Peña, Influence of the Wavelength on Laser Marking on ABS Filled with Carbon Black, Polymer-Plastics Technology and Engineering, pp. 1599-1607, Apr 2017, https://doi.org/10.1080/03602559.2017.1280735.

[16] C. Guo and S. C. Singh, Handbook of Laser Technology and Applications: Lasers Applications: Materials Processing and Spectroscopy, Volume 3, 2nd ed., p. 360, CRC Press, June 2021, https://doi.org/10.1201/9781315310855.

[17] Engraving lasers Rofin, Home page, [Online]. Available: https://graviranje.rs/Engraving_PORTAL/lasers/rofin/Rofin_PowerLine_F20.html [Accessed May 1, 2023].

[18] Olympus Global Homepage, [Online]. Available: https://www.olympus-global.com/news/2017/nr00633.html [Accessed May 1, 2023].